Void Fraction Measurements During Saturated Pool Boiling of Water on Partially Wetted Vertical Surfaces

S. P. Liaw
Student Mem. ASME

V. K. Dhir
Mem. ASME

Mechanical, Aerospace and Nuclear Engineering Department,
School of Engineering and Applied Science,
University of California,
Los Angeles, CA 90024-1597

Void fraction profiles adjacent to a vertical wall 6.3 cm wide and 10.3 cm high were measured during nucleate boiling. The experiments were conducted in saturated water at 1 atm pressure. In the experiments, the wettability of the surface was varied by controlling the degree of oxidation of the surface. Static contact angle was used as an indicator of the surface wettability. The void fraction was measured with a gamma densitometer. The experimental results show that the maximum void fraction occurs about 1–1.5 mm away from the heater surface. The wall void fraction, the maximum void fraction, and the thickness of the void layer increase with wall heat flux. It is found that for a given heat flux, the wall void fraction increases as the surface becomes less wettable, whereas the maximum heat flux decreases with increase in contact angle.

Introduction

Of all the modes of boiling, nucleate boiling is associated with the highest heat transfer coefficients. As a result, this process is of great interest with regard to applications as well as basic understanding. Numerous studies of nucleate boiling heat transfer have been reported in the literature. The results of these studies have generally been given in the form of correlations. So far, relatively few attempts have been made to describe the nucleate boiling process in a mechanistic way, and those efforts have met with little success. The primary cause for the very limited success of those attempts is a lack of understanding of the interaction of several surface and fluid parameters. To facilitate further development of mechanistic models of nucleate boiling and maximum heat fluxes, the purpose of the present work is to determine experimentally the interplay between the wall void fraction, surface wettability, and vapor flow dynamics away from the wall.

The earliest correlation for nucleate boiling is that of Rohsenow (1952). This correlation, though not based on sound reasoning of the physical mechanisms, has been very successful in predicting the observed nucleate boiling data. According to this correlation, the dependence of wall heat flux on wall superheat is written as

$$q = \mu_l h_{fg} \sqrt{\frac{g(\rho_l - \rho_v)}{\sigma}} \left(\frac{c_{pl} \Delta T}{C_s h_{fg}} \right)^m (\mathrm{Pr}_l)^{-n} \qquad (1)$$

In equation (1), the parameters C_s, m, and n are obtained empirically. The parameter C_s accounts for the effect of surface finish and wettability and as such varies with fluid-surface combination. The constants n and m have generally been found to vary between 3 and 4 for water. One reason for the success of this correlation is that it combines a correct length scale with appropriate thermophysical properties. Subsequent work has led to some modifications (Dwyer, 1974) of the above correlation but not in any significant way.

A prerequisite to the development of a mechanistic model for nucleate boiling is the delineation of various mechanisms by which energy can be transferred from the heater surface. It has generally been accepted that transient conduction and evaporation at nucleation sites and convection over the inactive regions of the heater are the relevant mechanisms. However, at higher heat fluxes, evaporation dominates over the two mechanisms. A comparison of the magnitudes of heat transfer rates associated with these mechanisms and related discussion is given by Hsu and Graham (1976).

Although most of the energy at high heat fluxes is transferred by evaporation, the location at which evaporation occurs at the bubble surface was a controversial topic in the 1960s. Two points of view have been that evaporation occurs over the upper surface of a bubble as opposed to underneath a bubble. Subsequent work lends credence to the earlier contention of Moore and Mesler (1961) that most of the evaporation occurs underneath the bubbles.

Apart from a detailed description of the modes of heat transfer, a mechanistic model also requires a knowledge of the site density as a function of wall superheat, vapor bubble size and its area of influence, bubble release frequency or superficial vapor velocity, and the vapor flow dynamics in the vicinity of the heater. The site density and bubble size and shape are strongly influenced by surface characteristics such as finish, wettability, cleanliness, etc. Because of the involvement of numerous variables and their interactions, the development of a totally mechanistic model for nucleate boiling has been an insurmountable task. Fath and Judd (1978) attempted to predict nucleate boiling heat flux on a mechanistic basis. However, they employed several of the parameters inferred from the experiments and as a result simply established the self-consistency of their model.

Further progress in the development of mechanistic models for nucleate boiling strongly depends not only on the correct modeling of the various transport processes but also on the parameters that characterize the heater surface and the fluid flow conditions away from the wall. In this context, the purpose of the present work is twofold:

(*i*) to determine the effect of surface wettability on nucleate boiling heat fluxes; and

(*ii*) to delineate the interaction between the boiling process at the wall and the vapor flow dynamics away from the wall. The second objective is met through the measurement of void profiles adjacent to the heated vertical wall. This study was designed to lay the ground work for our future efforts toward

Contributed by the Heat Transfer Division and presented at the ASME Winter Annual Meeting, Boston, Massachusetts, December 13–18, 1987. Manuscript received by the Heat Transfer Division September 24, 1987. Keywords: Boiling, Multiphase Flows.

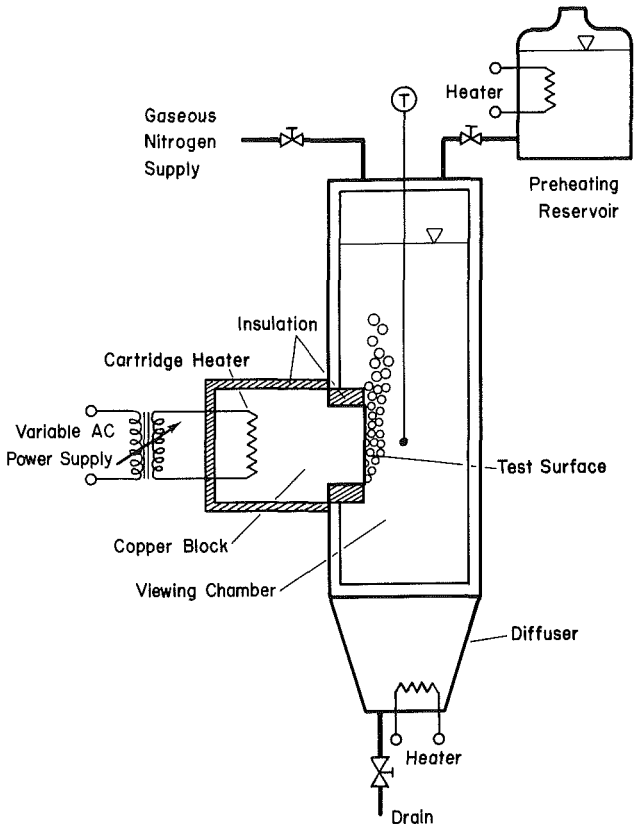

Fig. 1 Schematic diagram of the test setup for pool boiling study

development of a theoretical model for the complete boiling curve.

Experiments

The experimental apparatus used in this study was essentially the same as that described earlier by Bui and Dhir (1985) and by Liaw and Dhir (1986). Figure 1 shows a schematic diagram of the apparatus. The test surface is rectangular in shape and has a width of 6.3 cm and a height of 10.3 cm. The surface was machined from one end of a cooper rod having a purity of 99.9 percent. Eight cartridge heaters, four rated at 2 kW and the other four rated at 1 kW, are embedded in the copper rod. Thirty-gage chromel-alumel thermocouples are positioned along the vertical axis of the rectangular boiling surface at four locations, 8, 26, 52, and 77 mm from the lower edge. At each vertical location, four thermocouples were embedded at various depths normal to the boiling surface. The test section is mounted on one side of a viewing and liquid holding chamber. Glass plates are placed on the remaining three sides of the chamber for simultaneous observation of the front and side views of the boiling phenomena on the test surface. The liquid holding and viewing chamber is a square duct with a 14 cm by 14 cm cross section.

Startup of a typical experimental run began with deaeration of the test liquid by vigorous boiling in a reservoir and with preheating of the test section. The chamber was then filled with the test liquid from the reservoir and the boiling process was commenced. The power to the heaters was controlled with an autotransformer and was determined by voltmeter and ammeter readings. A steady-state condition was assumed to exist when the temperature of the test section changed less than 1 K in 5 min. All of the tests reported in this work were carried out in a steady-state mode. For these tests, the thermocouple output was recorded directly on a Fluke data logger. The wall heat flux was determined by knowing the temperature gradient, which was linear through the copper block except near the edges. The surface temperature was obtained by extrapolating the known temperature profile at a given vertical location. A balance between the energy input in the cartridge heaters and the energy lost at the boiling surface and the copper block surface was also made. At a boiling surface heat flux of 74 W/cm^2, the calculated energy loss rate agreed to within 5 percent of the energy input rate.

Surface Preparation and Measurement of Contact Angles. A well-defined procedure already described in detail (Liaw and Dhir, 1986) was used to obtain surfaces of different degrees of wettability. In this procedure, the polished surface of a copper disk (secondary surface) was heated in air while increasing the surface temperature at about 6 K/min until the surface temperature reached a desired value. The surface was then maintained at that temperature for a predetermined period and was subsequently cooled at a rate of about 2 K/min to the temperature at which the contact angle was to be measured. The inset in Fig. 2 shows the surface oxidation procedure. Thereafter a liquid droplet 0.2 cm^3 in volume was placed on the test surface. The initial temperature of the droplet was the same as the test surface. The contact angle was determined from a photograph of the droplet placed on the test surface. Figure 2 shows the contact angles measured at room temperature as a function of the maximum temperature to which the secondary surface was heated. To obtain a desired degree of wettability of the primary test surface, the same procedure as described above was repeated. To assure that the surface conditions were indeed duplicated, in one instance the contact angles on the secondary and the primary surface were measured and found to be within the measurement uncertainty, which was about ±3 deg.

Nomenclature

C_1, C_2 = constants
C_s = empirical constant characterizing a surface
c_{pl} = specific heat of liquid
g = gravitational acceleration
h_{fg} = latent heat of vaporization
I = beam intensity
I_g = beam intensity after it passes through gas or vapor
I_l = beam intensity after it passes through liquid
L = spacing of vapor stems
l = thermal layer thickness
Pr_l = Prandtl number of liquid
q = heat flux
T_{sat} = saturation temperature of liquid
T_w = wall temperature
U_c = vapor velocity in a continuous passage
$\bar{U}_c$ = average vapor velocity in the continuous passages
U_H = Helmholtz critical velocity
U_t = terminal velocity of a bubble
$\bar{U}_v$ = superficial velocity of vapor
x = distance normal to the wall
z = distance along the wall
z' = dimensionless distance along the wall
α = void fraction
α_{max} = maximum void fraction at wall
α_w = void fraction at wall
γ = ratio of width of test surface to width of test chamber
ΔT = wall superheat
$\bar{\delta}$ = effective vapor layer thickness
μ_l = viscosity of liquid
ρ_l = density of liquid
ρ_v = density of vapor
σ = surface tension
ϕ = contact angle

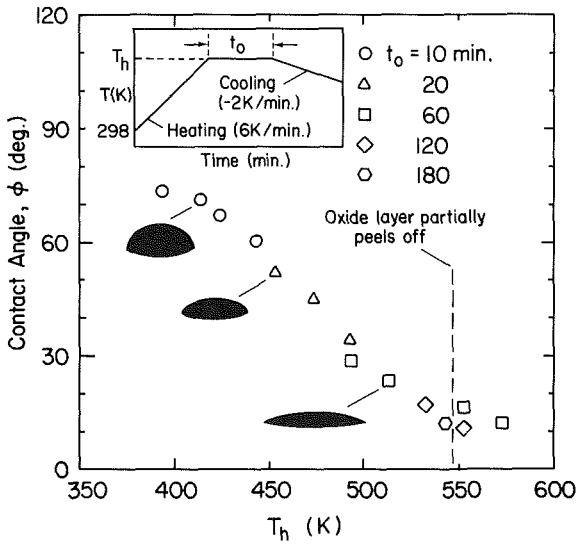

Fig. 2 Dependence of the contact angle measured at room temperature on the highest temperature attained during oxidation (the dark symbols are photographs of droplets)

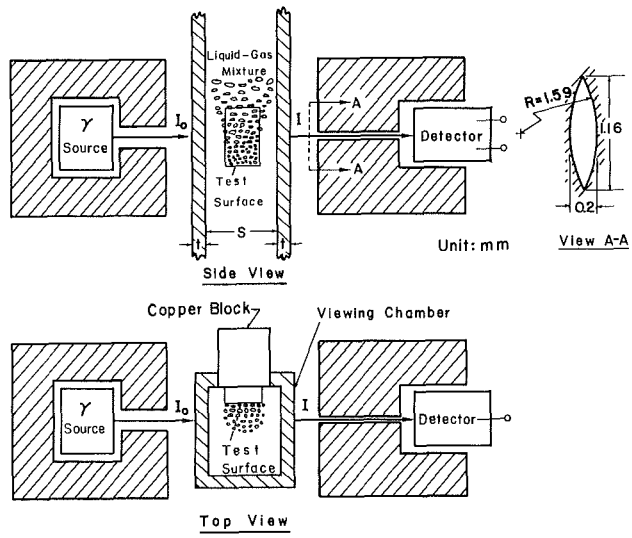

Fig. 3 Schematic diagram of orientation of gamma beam with respect to test surface

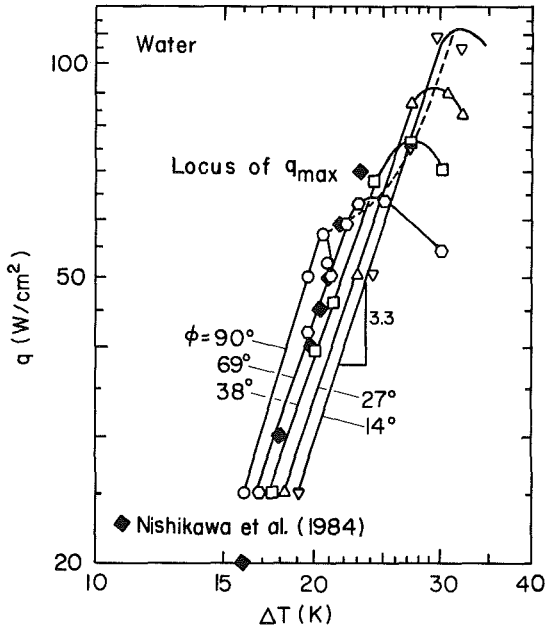

Fig. 4 Variation of heat flux with wall superheat for various contact angles

Void Fraction Measurement. The void fraction profiles adjacent to the boiling surface were obtained with a gamma densitometer. Figure 3 shows the orientation of the gamma beam with respect to the surface. The gamma densitometer consists of a 150-milli-Curie cesium-137 source and a NaI detector, both encased in lead. The diameter of the source collimeter is 6.25 mm (1/4 in) and that of the detector is 3.18 mm (1/8 in). The source and the detector are placed 0.62 m (2 ft) apart on a base plate, which in turn is mounted on a lift truck. The base plate is moved vertically upward or horizontally across the test surface by rotating threaded spindles. In this way the beam can be made to traverse the test section at several horizontal and vertical locations along the plate. After passing through the test chamber the gamma beam is absorbed in the detector and produces a pulsed signal. The circular area over which the signal is received and the area of the detector are experimentally found to have an eccentricity of about 2.9 mm. As such, the pulsed signal is representative of nearly point value of the void fraction rather than an average over the cross-sectional areas corresponding to the source or the detector. The signal magnitude was analyzed and sorted in an HP model 401D pulse analyzer. The signal output was printed on a TMC model 500A printer.

Prior to the measurement of void fractions on the boiling surface, calibration for the attenuation of the beam intensity was made when the test section had only air or water in it. The density of air is not much different from that of water vapor. As a result little error (0.03 percent) is made in assuming that attenuation of beam intensity in water vapor will be the same as in air. If γ is the ratio of the width of the test surface to that of the test chamber (see Fig. 3), the average void fraction across the cross section of the surface can be written as

$$\alpha = \gamma \frac{\ln(I/I_l)}{\ln(I_g/I_l)} \tag{2}$$

The variability in the void fraction due to uncertainty in the value of I is calculated to be ± 1.4 percent. All of the distances normal to the wall were measured from the test surface. The position of the test surface ($x=0$) was established by aligning the centerline of the gamma beam with the test surface. The beam center was assumed to be tangent to the surface when the rate at which attenuation of the beam intensity was maximum. The uncertainty in location of the surface is estimated to be 0.05 mm. This introduces a calibration error as well as an error in the measured void fraction. The total error in the void fraction as a result of statistical error (± 1.4 percent) as stated earlier, and taking into account the uncertainty in the location at which the void fraction is measured, is calculated to be less than ± 0.05 at 0.4 mm from the surface. Since the uncertainty in the measured void fractions at distances shorter than 0.4 mm was large, all of the reported data were limited to distances greater than 0.4 mm from the surface. The error in void fraction, however, decreases with distance from the wall and is calculated to be ± 0.03 at 20 mm from the wall.

The wall void fractions were determined by extrapolation of the data obtained at locations farther than 0.4 mm from the wall. The maximum uncertainty in the wall void fraction is found to be ± 0.06 and was obtained by extrapolating the mean and upper and lower bounds of the data representing the void profiles at distances greater than 0.4 mm from the wall. It

Table 1 Values of C_s for different contact angles

ϕ,deg	C_s
14	0.0209
27	0.0202
38	0.0194
69	0.0186
90	0.0172

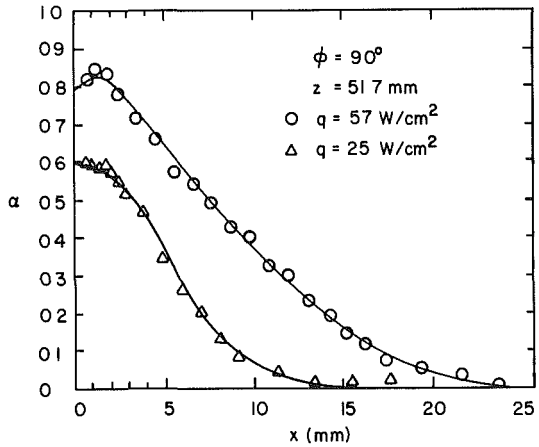

Fig. 5 Void profiles at midplane of the test surface for a contact angle of 90 deg

should be stressed here that for well-wetted surfaces the interface shape could change rapidly very near the wall. For these surfaces the uncertainty in the wall void fraction could conceivably be higher than that evaluated in this work.

Results and Discussion

The nucleate boiling data were obtained under steady-state conditions at a system pressure of 1 atm with saturated water as the test liquid. The reported void fractions represent an average over the width of the plate and over time. The reported heat transfer data were obtained under steady-state conditions.

Figure 4 shows dependence of nucleate boiling heat flux on wall superheat for contact angles of 90, 69, 38, 27, and 14 deg. The reported data are for the higher end of nucleate boiling and no attempt was made to obtain data near inception of nucleate boiling. In all cases, the dependence of wall heat flux on wall superheat is similar, i.e., $q \sim \Delta T^{3.3}$. However, as the surface wettability improves, the approach to maximum heat flux becomes gradual and a higher superheat is required to attain the same heat flux. The maximum heat flux nevertheless increases as the surface wettability improves. Although it is not the purpose of this work to develop a correlation, it is found that the constant C_s in Rohsenow's equation (1) varies almost linearly with contact angle. The values of C_s are given in Table 1. In Fig. 4, the data of Nishikawa et al. (1984) for saturated water at one atmosphere pressure boiling on a copper plate are also plotted. The contact angle of water with polished copper is 90 deg. It is seen that their data lie between the 69 and 90 deg data obtained in the present work. Their data also show the same dependence of heat flux on wall superheat as do the present data. It should also be mentioned that at high nucleate boiling heat fluxes, Nishikawa et al. observed little effect of the orientation of the heater surface.

Figure 5 shows the wall void fraction profiles at the midplane of the test surface for a contact angle of 90 deg and for heat fluxes of 25 and 57 W/cm^2. At both heat fluxes, the

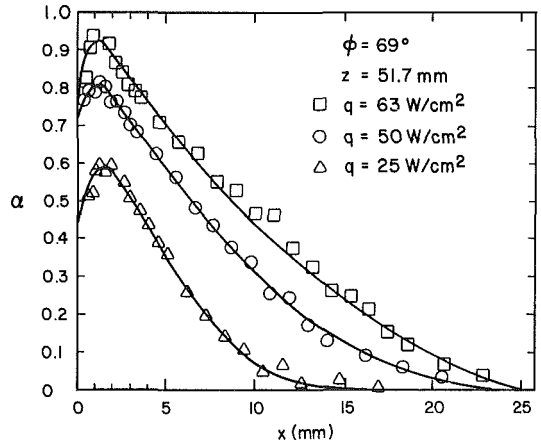

Fig. 6 Void profiles at midplane of the test surface for a contact angle of 69 deg

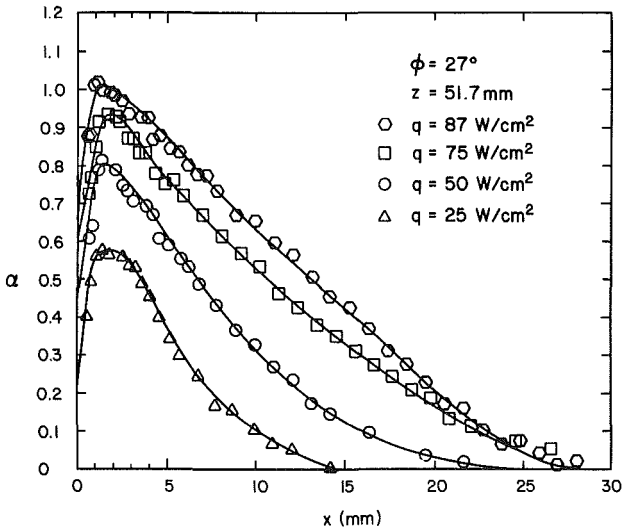

Fig. 7 Void profiles at midplane of the test surface for a contact angle of 27 deg

void fraction is nearly constant in the region immediately next to the wall. Thereafter it decreases nearly exponentially. The wall void fraction and thickness of the voided region increase with heat flux. Figures 6 and 7 show the midplane void profiles for contact angles of 69 and 27 deg. General features shown by these profiles are similar to those observed earlier for a contact angle of 90 deg. However, for contact angles less than 90 deg, the maximum void fraction occurs at about 1 to 1.5 mm away from the wall. For a given contact angle, the steepness of the profile appears to be independent of heat flux. However, the steepness increases with decrease in contact angle. This is a clear manifestation of the shape of the interface near the heater surface.

It is also noted that for contact angles less than 90 deg, the location of maximum void fraction shows little change as heat flux is increased. Another interesting observation that can be made from Figs. 5, 6, and 7 is that though in each case the highest heat flux is very close to the maximum heat flux for that contact angle, the maximum void fraction is never equal to unity except when the heat flux is 87 W/cm^2 for a contact angle of 27 deg. Since in the absence of a void fraction equal to unity, liquid is always available, the maximum heat flux must then be caused by some limitation occurring at the surface itself. In fact, a detailed theoretical investigation of the

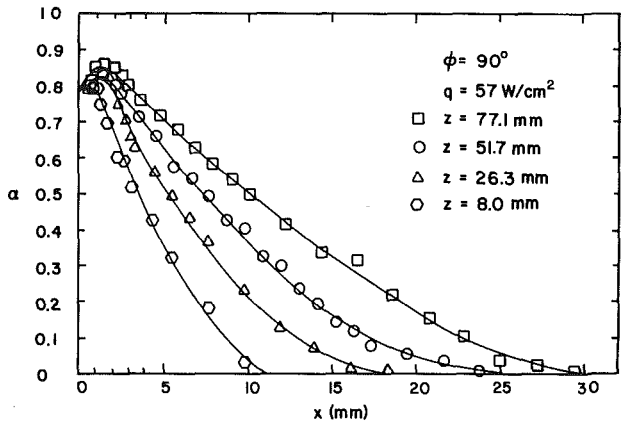

Fig. 8 Void profiles at several vertical locations for a contact angle of 90 deg

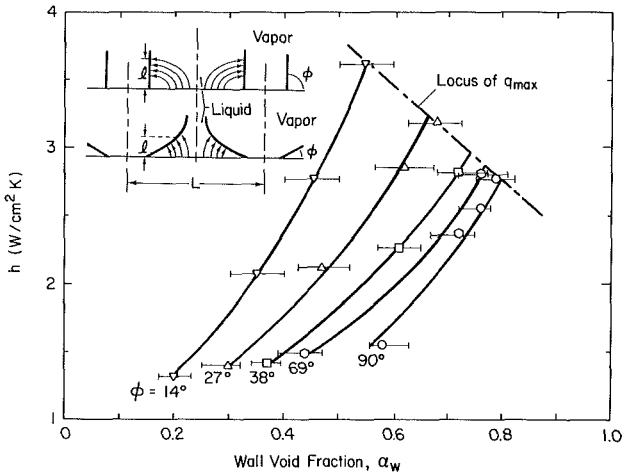

Fig. 10 Heat transfer coefficient as a function of wall void fraction for several contact angles

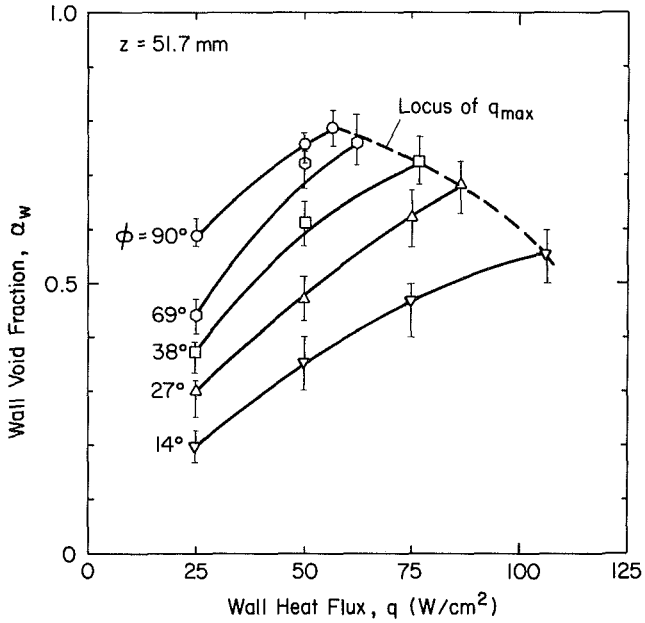

Fig. 9 Dependence of wall void fraction on wall heat flux

surface limited maximum heat flux is the topic of the companion paper. Occurrence of a void fraction of unity implies formation of a continuous vapor layer away from the surface. The continuous vapor layer inhibits the flow of liquid to the surface, hence leading to a critical heat flux condition. Thus it appears that a heat flux of 87 W/cm² for a contact angle of 27 deg represents a demarcation between surface-controlled maximum heat flux and that controlled by vapor flow dynamics away from the surface.

The void fractions as a function of distance from the bottom edge of the vertical plate are plotted in Fig. 8. The plotted data are for a contact angle of 90 deg and for a heat flux very near the maximum heat flux. The wall void fraction is observed to be independent of the vertical distance. This is consistent with the observed uniformity of the wall heat flux and the temperature along the plate. The maximum void fraction increases slightly with distance but there is a large increase in the extent of the voided region with distance. This is mainly because of addition of vapor along the direction of flow. It should be noted that in order to avoid clutter, the variability in the measured void fractions has not been shown in Figs. 5–8.

The wall void fractions obtained by extrapolating the profiles such as those shown in Figs. 5, 6, and 7 are plotted in Fig. 9 as a function of wall heat flux. For all of the contact angles, the wall void fractions increase with heat flux. Near the maximum heat flux condition, the wall void fraction for all the contact angles lies between 0.55 and 0.8. Since the plotted void fractions are averaged over time and width of the plate, they represent the dry fraction of the heater at a given instant.

Before proceeding further, it is pertinent to compare the void fractions measured in the present work with the data reported in the literature. Earlier attempts to measure void fractions during nucleate and/or transition boiling are those of Iida and Kobayasi (1969), Hasegawa et al. (1973), Ragheb and Cheng (1979), Nishikawa et al. (1984) and Dhuga and Winterton (1985). Both Iida and Kobayasi and Hasegawa et al. used a 0.04-mm-dia movable probe to measure the void fractions in the vicinity of a 2.9-cm-dia horizontal disk. Distilled water was used as the test liquid. Surprisingly, in both cases the maximum heat flux was only 25 W/cm². Because of lack of information on the contact angles in these studies, it is difficult to make a meaningful comparison of the measured void fractions. Nevertheless if a contact angle of 69 deg is assumed, in the present work the mean values of α_w and α_{max} at a heat flux of 25 W/cm² are found to be 0.44 and 0.6, respectively. In comparison, Iida and Kobayasi and Hasegawa et al. measured void fractions of 0.53 and 0.71, respectively, at 0.1 mm away from the wall. The maximum void fractions in the two studies were 0.94 and 0.85, respectively, and occurred at 0.5 to 1.0 mm away from the wall.

Ragheb and Cheng (1979) used a 1.02-mm zirconium wire embedded in a copper block to measure the fractional surface area occupied by liquid during subcooled forced flow transition boiling. In their work the void fraction measured at the maximum heat flux was only 0.15 to 0.2. Similar values of void fraction near the maximum heat flux on a horizontal plate have been reported by Dhuga and Winterton (1985). Nishikawa et al. (1984) used an electric probe to measure void fraction at 0.5 mm away from the heated plates oriented at different angles to the vertical. For their nucleate boiling data, which were plotted earlier in Fig. 4, a mean void fraction at a heat flux of 25 W/cm² is found to be 0.58. This value is very close to the value obtained in the present work at 0.5 mm from a surface with a contact angle of 69 deg.

In Fig. 10, the heat transfer coefficients are plotted as a function of wall void fraction for contact angles of 14, 27, 38, 69, and 90 deg. From the plotted data, it is seen that for a fixed void fraction, the heat transfer coefficient increases as the contact angle decreases or the surface becomes more wet-

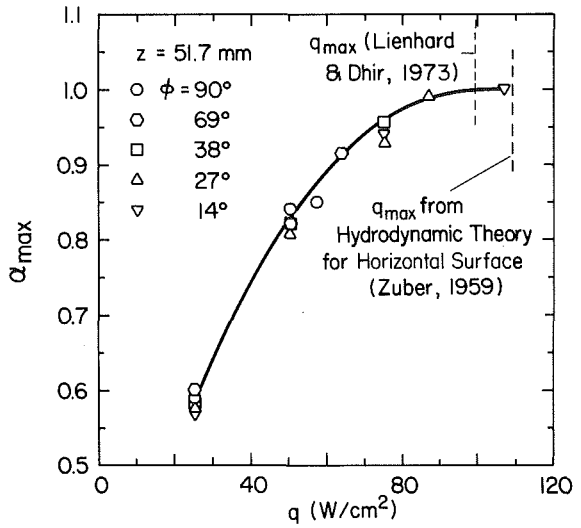

Fig. 11 Maximum void fraction as a function of heat flux for several contact angles

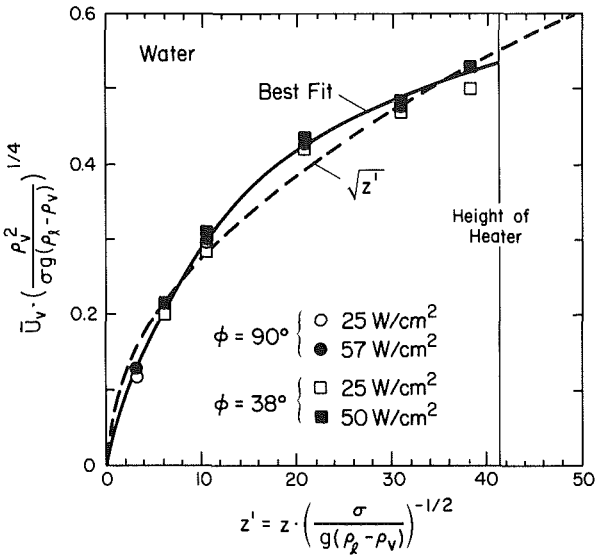

Fig. 12 Dependence of superficial vapor velocity on dimensionless distance from the leading edge

table. Since transport of energy occurs at the heater surface, one can infer that for a fixed wall void fraction an increase in heat transfer coefficient as the contact angle becomes small implies thinning of the liquid layer intervening between the vapor–liquid interface and the wall. This is shown qualitatively in the inset in Fig. 10. The inference drawn here also implies that it is the evaporation of the liquid layer (macro/micro) adjacent to the wall that controls the vapor volume flux leaving the heater.

The maximum void fraction for all of the contact angles is plotted in Fig. 11 as a function of wall heat flux. The maximum void fraction is seen to become unity as the observed heat fluxes approach those given by the hydrodynamic theory. Contrary to the wall void fraction, the maximum void fraction is found to be independent of the contact angle. The maximum void fraction depends only on the magnitude of the vapor volume flux leaving the heater or conceivably on the vapor flow behavior in the pool. The location of maximum void fraction thus represents the boundary beyond which flow dynamic effects dominate. This is elaborated further in the following paragraphs.

Vapor Flow Dynamics

An assessment of vapor flow behavior away from the heater surface is made from the observed superficial velocity of the vapor. The observed superficial velocity of vapor is compared with the terminal velocity of a single bubble, the vapor velocity in a continuous passage, and the critical velocity for Kelvin-Helmholtz instability of a vapor jet. If an effective vapor layer thickness is defined as

$$\delta = \int_0^\infty \alpha \, dx \tag{3}$$

the vapor superficial velocity at a vertical location z can be written as

$$\bar{U}_v = \frac{qz}{\rho_v h_{fg} \delta} \tag{4}$$

The terminal velocity of a bubble or slug of vapor can be written by balancing liquid inertia with the buoyancy force on a bubble as

$$U_t = C_1 \sqrt[4]{\frac{\sigma g(\rho_l - \rho_v)}{\rho_l^2}} \tag{5}$$

where the constant C_1 is generally assigned a value of 2.9 (see Lahey and Moody, 1977) for churn turbulent bubbly flow. On the other hand, for an inviscid vapor the velocity in a continuous passage surrounded by an inviscid liquid is obtained by balancing the hydrostatic head with the inertia of the vapor as

$$U_c = \sqrt[4]{\frac{\sigma g(\rho_l - \rho_v)}{\rho_v^2}} \sqrt{2z'} \tag{6}$$

where z' is defined as

$$z' = z \Big/ \sqrt{\frac{\sigma}{g(\rho_l - \rho_v)}} \tag{7}$$

and is measured from the location at which vapor starts to move in the vertical direction. The characteristic length used in equation (7) was also used to define the diameter of the bubble while obtaining equation (5). Since vapor is added to the pool uniformly along the plate, the average vapor velocity in the jets along the plate can be obtained by integrating equation (6) as

$$U_c = 0.94 \sqrt[4]{\frac{\sigma g(\rho_l - \rho_v)}{\rho_v^2}} \sqrt{z'} \tag{8}$$

z' is measured from the leading edge of the plate.

The critical velocity at which a vapor jet with axis parallel to the gravitational acceleration becomes Helmholtz unstable can be written (see Lamb, 1945) as

$$U_H = C_2 \sqrt[4]{\frac{\sigma g(\rho_l - \rho_v)}{\rho_v^2}} \tag{9}$$

where the constant C_2 is of the order of unity. In writing equation (9) the diameter of the jet is assumed to be proportional to the characteristic length used in equation (7).

The average superficial velocity calculated from equation (4) is plotted as a function of vertical distance in Fig. 12. The velocity has been nondimensionalized with the characteristic velocity in equations (8) or (9). The superficial velocity is found to increase as the square root of the distance from the leading edge and is independent of the magnitude of the heat flux and the contact angle. The independence of the super-

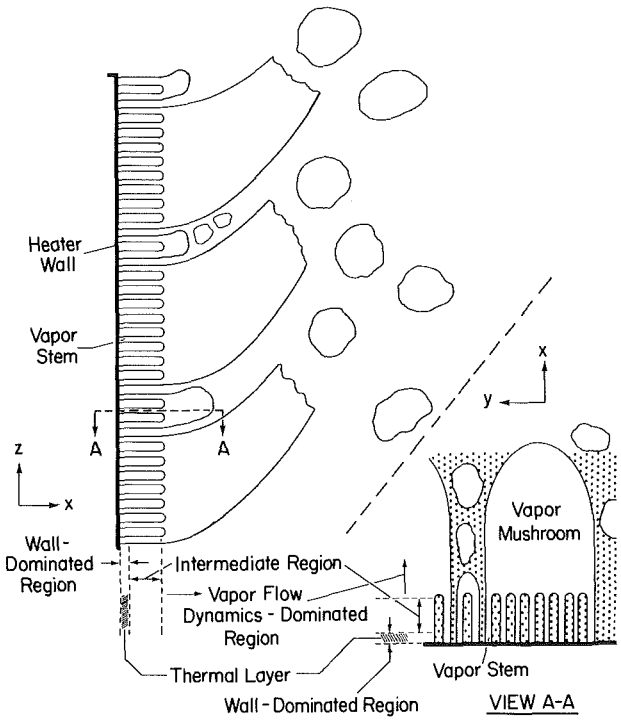

Fig. 13 Conceptualization of three regimes during pool boiling on a vertical surface for a contact angle of 90 deg

ficial vapor velocity from the contact angle is indicative of the fact that conditions on the wall do not influence the flow behavior away from the wall. The nondependence of vapor velocity on heat flux implies that once the vapor velocity reaches a certain allowable value, more vapor flow passages develop to accommodate a higher vapor volume flux. As a result, the flow area or $\bar{\delta}$ increases with heat flux. Although the observed superficial velocity shows the same dependence on distance from the leading edge as is given by equation (8), the observed velocity is about an order of magnitude smaller than that predicted from equation (8). This is not unexpected since all of the flow area is not occupied by vapor jets. The observed maximum velocity at the top of the vertical plate is about eight times higher than that given by equation (5) for the terminal velocity of a bubble. This suggests that a large fraction of vapor definitely moves through continuous vapor passages. The most probable location of these passages is the region close to the wall. Although, according to equation (8), vapor velocity in the jets could continue to increase indefinitely with distance, the upper limit on the average superficial velocity will be set by equation (9).

It should be stressed here that the above evaluation does not represent a model of the vapor flow dynamics but an assessment of the prevailing vapor flow configurations.

From the results presented above, the boiling phenomenon on a heater surface can be subdivided into three regions. The region strongly influenced by the wall characteristics extends up to the outer edge of the thermal layer, which as shown in the companion paper has a thickness of the order of 10^{-5} m. The vapor flow dynamics dominates the region beyond the location at which maximum void fraction occurs. The maximum void fraction occurs at about 10^{-3} m away from the wall. The intermediate region between the outer edge of the thermal layer and the location at which α_{max} occurs is influenced by both the wall and the vapor flow dynamics away from the wall. Figure 13 shows the conceptualization of the process.

For partially wetted surfaces, $\phi > 27$ deg, the maximum heat flux condition occurs as a result of the limitation on the energy that can be removed from the liquid-occupied region of the heater. For these surfaces, the void fraction in the vicinity of the surface is always less than unity. Hence liquid has an easy access to the surface. The maximum as well as the nucleate boiling heat fluxes are only weakly affected by the flow conditions away from the wall as long as vapor can find its way out of the wall region unhindered.

For relatively well-wetted surfaces, $\phi < 20$ deg, the vapor flow dynamics away from the surface may control the maximum heat flux. In the present study, the data point for $\phi = 27$ deg appears to approach that limiting condition, whereas the surface with $\phi = 14$ deg appears to meet that condition. From these data points, it is found that at maximum heat flux on well-wetted surfaces the void fraction away from the wall reaches a value of unity. At a void fraction equal to unity, an obstruction to the flow of liquid to the interior regions of the vertical wall can develop. This condition appears to be analogous to what has been assumed in the past with respect to hydrodynamically controlled boiling crisis in pool boiling. In the hydrodynamic theory originally proposed by Zuber (1959), it was assumed that the maximum heat flux occurs when vapor escape velocity and vapor flow area fraction reach their critical values. A critical value can be assigned to the average vapor layer thickness $\bar{\delta}$ when maximum void fraction reaches unity. The present observations, however, show that local vapor velocity attains its maximum value at relatively low heat fluxes and remains constant thereafter.

A void fraction of unity slightly away from the heater may be a preferable criterion for maximum heat fluxes on well-wetted surfaces. This criterion will eliminate separate specification of average vapor velocity and fractional vapor flow area. Such a criterion will also provide a natural link between pool and forced flow boiling since void fraction can be related to the drift velocity in both cases. To develop a totally analytical model for nucleate and transition boiling, attention needs to be paid to all of the three regions identified in this work and as shown in Fig. 13. The maximum heat flux and the corresponding wall superheat will be a natural outcome of such an analysis.

Summary and Conclusions

1 The effect of surface wettability on nucleate boiling and maximum heat fluxes has been quantified.

2 Void fractions adjacent to a heated vertical wall have been measured for several heat fluxes and contact angles.

3 At a given heat flux, the wall void fraction is found to be sensitive to contact angle. For the contact angles studied in this work, the data suggest wall void fractions of 55–80 percent at the onset of maximum heat flux condition.

4 For contact angles less than 90 deg, the maximum void fraction occurs at about 1–1.5 mm away from the wall and is found to be independent of contact angle.

5 The void fraction everywhere in the vicinity of the surface is found to be less than unity at maximum heat flux for all of the surfaces except the surfaces with $\phi = 27$ and 14 deg. This confirms that for partially wetted surfaces the maximum heat flux condition is controlled by surface effects.

6 Based on the observations, the boiling phenomenon on a heater is subdivided into three regions: the wall-dominated region, the vapor flow dynamics dominated region, and the intermediate region.

Acknowledgments

This work received support from the NSF under Grant No. CBT-84-17684.

References

Bui, T. D., and Dhir, V. K., 1985, "Transition Boiling Heat Transfer on a Vertical Surface," ASME JOURNAL OF HEAT TRANSFER, Vol. 107, pp. 756–763.

Dhuga, D. S., and Winterton, R. H. S., 1985, "Measurement of Surface Contact Transition Boiling," *Int. J. Heat Mass Transfer*, Vol. 28, pp. 1869–1880.

Dwyer, O. E., 1974, *Boiling Liquid Metal Heat Transfer*, American Nuclear Society, Hinsdale, IL.

Fath, H. S., and Judd, R. L., 1978, "Influence of System Pressure on Microlayer Evaporation Heat Transfer," ASME JOURNAL OF HEAT TRANSFER, Vol. 100, pp. 49–55.

Hasegawa, S., Echigo, R., and Takegawa, T., 1973, "Maximum Heat Fluxes for Pool Boiling on Partly Ill-Wettable Heating Surfaces," *Bulletin of JSME*, Vol. 16, No. 97, pp. 1076–1084.

Hsu, Y. Y., and Graham, R. W., 1976, *Transport Processes in Boiling and Two-Phase Systems*, McGraw-Hill, New York.

Iida, Y., and Kobayasi, K., 1969, "Distribution of Void Fraction Above a Horizontal Heating Surface in Pool Boiling," *Bulletin of JSME*, Vol. 12, No. 50, pp. 283–290.

Lahey, R. T., and Moody, F. J., 1977, *The Thermal Hydraulics of a Boiling Water Nuclear Reactor*, American Nuclear Society, Hinsdale, Illinois.

Lamb, H., 1945, *Hydrodynamics*, 6th ed., Dover Publications Inc., New York.

Liaw, S. P., and Dhir, V. K., 1986, "Effect of Surface Wettability on Transition Boiling Heat Transfer From a Vertical Surface," *Proc. Eighth Int. Heat Transfer Conference*, Vol. 4, pp. 2031–2036.

Moore, F. D., and Mesler, R. B., 1961, "The Measurement of Rapid Surface Temperature Fluctuations During Nucleate Boiling of Water," *AIChE J.*, Vol. 7, No. 4, pp. 620–624.

Nishikawa, K., Fujita, Y., Uchida, S., and Ohta, H., 1984, "Effect of Surface Configuration on Nucleate Boiling Heat Transfer," *Int. J. Heat Mass Transfer*, Vol. 27, pp. 1559–1571.

Ragheb, H. S., and Cheng, S.C., 1979, "Surface Wetted Area During Transition Boiling in Forced Convective Flow," ASME JOURNAL OF HEAT TRANSFER, Vol. 101, pp. 381–383.

Rohsenow, W. M., 1952, "A Method of Correlating Heat Transfer Data for Surface Boiling of Liquids," *Trans. ASME*, Vol. 74, pp. 969–976.

Tong, L. S., 1978, "Heat Transfer in Reactor Safety," *Proc. Sixth Int'l. Heat Transfer Conf.*, Vol. 6, pp. 285–309.

Zuber, N., 1959, "Hydrodynamic Aspects of Boiling Heat Transfer," Ph.D. dissertation, University of California, Los Angeles; also published as U.S. Atomic Energy Commission Report No. AECU-4439.